Repair of Closed Fermentation Chamber and Its Influence on Strength Properties of the Tank – Case Study

Bogdan Szturomski[1], Radosław Kiciński[1], Aneta Szturomska[1], Jacek Krawczyk[2]

[1] Mechanical and Electrical Engineering Faculty, Polish Naval Academy, ul. Inżyniera Jana Śmidowicza 69, 81-127 Gdynia, Poland
[2] LIT S.C. Aleja Niepodległości 863A, 81-861 Sopot, Poland
* Corresponding author's e-mail: r.kicinski@amw.gdynia

ABSTRACT

The paper shows research on a closed fermentation chamber (CFC) that is an element of the Biogas Combined Heat and Power Plant located in the Gdańsk East Sewage Treatment Plant. This tank is mounted as an above-ground cylinder-shaped structure covered with a cone-shaped roof. Corrosion and leaks appeared in the tanks during many years of operation. In this work, it was decided to investigate their cause and propose a method of counteracting them. The article presents the research on the influence of individual operational and environmental loads on the stress distributions in the tank structure. Numerical simulations using the Finite Element Method were carried out for shell and solid models. Moreover, the stress distributions in cylindrical steel tanks were compared depending on the shape of the chamber top. The research results allowed us to identify the design errors of the closed fermentation chambers. It finds out that the connection of the cylindrical part of the tank with the conical roof requires reinforcement. A tank repair technology using Belzona composites was proposed to modify the joint geometry. A simulation was performed, taking into account the proposed repair technology. Its results showed a reduction of stresses compared to the state before repair by 19%.

Keywords: finite element method, computational mechanics, repair technology.

INTRODUCTION

Unstable crude oil prices or ecological aspects related to reducing carbon dioxide emissions into the atmosphere contributed to the search for new energy sources. Biogas CHP plants are one of the technologies of new electricity sources [1].

The production of biogas is a technology used primarily for the production of renewable energy, as well as for the valorization of organic residues. Biogas is the end product of the anaerobic digestion process in which microorganisms decompose organic matter. It consists mainly of methane and carbon dioxide and may contain small amounts of hydrogen sulphide, hydrogen, water, carbon monoxide and siloxanes. Methane, hydrogen and carbon monoxide can be burned or oxidized, releasing energy, which allows the use of biogas as fuel [1–3]. This process was widely used in households providing heat and electricity. Nowadays, the biogas sector is growing rapidly and cutting-edge developments are laying the foundations for creating biogas plants as advanced bio-energy plants [4].

One of such bio-power plants is the "Gdańsk-Wschód" sewage treatment plant. As a result of wastewater treatment in the "Gdańsk-Wschód" treatment plant, sewage sludge is produced, which is fed to the fermentation chambers, where the process of methane sludge fermentation takes place. The biogas produced during fermentation, after purification, is used for the energy needs of the sewage treatment plant, i.e. burned in a local gas-oil boiler plant [5].

In 2012, the CHP (Combined Heat and Power Plant) were launched at the Gdańsk East Wastewater Treatment Plant. This investment allowed for the reduction of energy consumption from

non-renewable sources and the reduction of greenhouse gas emissions. The construction of CHP was carried out as part of the project entitled "The energy use of biogas at the Gdańsk East Sewage Treatment Plant", co-financed by the Regional Operational Program for the Pomeranian Voivodeship for 2007–2013. The installation is powered by biogas produced in closed fermentation chambers (CFC), fuel for the internal combustion engine that drives the electric current generator [6].

During the modernization, the contractor decided to use a ready-made structure, which is grain silos. The silo should meet not only the requirements of European standards in terms of strength and stability of the structure. It is important at the design stage to also anticipate the impact of nonstandard conditions. However, before considering the "unusual" loads that may be subjected to the structure of the silo, basic strength and stability calculations should be performed [7]. These tanks are not designed to work under pressure. The constructors were probably aware of a stress concentration in the connection between the wall and the roof. Therefore, the structure has been stiffened by using a 300´100 channel section. This procedure disturbed the stiffness proportions due to the combination of a thin steel sheet with a massive profile. Therefore, after several years of operation, leakages caused by corrosion appeared in them. The historical analysis of similar structures has shown that corrosion may not take place if there are cereal products in them. The presented analysis shows the fully rusty tanks, which were excluded from operation [8]. In the case under consideration, corrosion occurred only at the reinforcement of the tanks.. Many methods of diagnosing the causes of corrosion require the collection of appropriate specimens for testing. There are electrochemical tests, voltaperometric methods, electrochemical impedance spectroscopy, salt spray tests and hydrogen degradation. Unfortunately, destructive tests were not allowed as it would have violated the structure of the facility. Therefore, having the knowledge of literature and experience, analyzing the nature of the phenomenon and the environment in which the object works (acidic atmosphere, elevated temperature, electrolyte), it was assumed that it could be the result of electrochemical and stress corrosion. A series of numerical simulations using FEM was carried out to confirm this thesis. Computer

simulations are currently the basis of engineering activities, they are used to design structures and select materials [9], optimize existing structures [10] or diagnose the causes of damage. In the case under consideration, it was assumed that the damage to the tank was caused by stress corrosion cracking. It was decided to use the simulation to find the cause of the stress in the studied area.

RESEARCH OBJECT

The facilities working on the site of the sewage treatment plant are the product of the English company Permastore. This company produces universal tanks in the Glass-Fused-to-Steel technology, i.e. steel panels covered with cobalt glass embedded in the surface as a modular structure that theoretically allows the tank's design to any user's needs. They are used for the storage of loose and liquid materials in agriculture, industry and municipal services – for example, as process tanks, storage tanks for drinking water, sewage or sludge, generally for applications where there are no requirements for gas tightness and the tank does not work under additional pressure above the liquid surface. This is due to the way the cylindrical shell of the tank is closed through the conical roof. The bottom of the CFC is made of reinforced concrete in the shape of an inverted truncated cone with an inclination angle of 45° and is also the foundation for the steel tank structure. The chamber's ceiling is a truncated cone of sheets as above, with a slope angle of 15°. The tanks in the steel and reinforced concrete part (protruding above the ground) are protected with thermal insulation made of mineral wool covered with a corrugated sheet. Steel structure dimensions [11,12]:
- diameter – 22.20 m;
- height of the cylindrical part – 14.7 m;
- diameter of the flat part of the upper floor – 6.00 m;
- roof slope angle – 15°.
- Dimensions of the reinforced concrete part:
- height – 8.75 m;
- diameter of the flat part of the bottom – 3.20 m.

The sheathing of the steel part of the tank consists of 11 so-called "carg" (Figure 1). Cargs – these are belts made of steel sheets of varying thickness from 3.8 mm to 9.2 mm in height, connected with overlapping screws. The
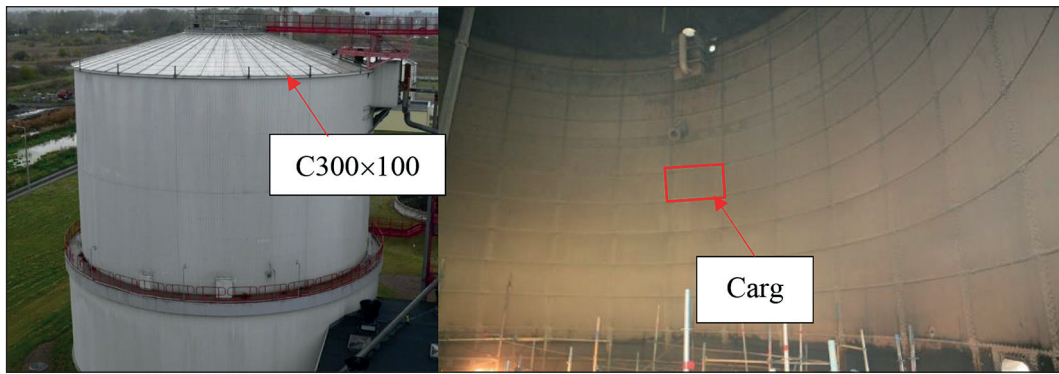
Figure 1. Closed Fermentation Chamber CFC for methane production (on left)
and its interior (on right). One of the cargs is shown in a red rectangle

roof sheathing is made of 7.3 mm thick sheet steel. The connections are sealed with rubber.

The tank's structure at the junction of the cylindrical part with the conical roof is reinforced with 26 sections of C-profiles 300´100 channels with a radius of curvature of the cylindrical part. C-profiles are connected to each other by flat bars twisted with screws. Twenty mm wide expansion gaps are provided between the C-profiles. The roof structure is radially reinforced with 5 mm thick steel profiles. Details of the tank bindings are shown in Figure 2.

As a result of many years of operation, there is a local loss of tightness on the circumference of the upper cylindrical part at the contact with the conical dome. The cause of the leakage is corrosion pitting that occurs around the entire circumference of the tank in the structure of the tank reinforcing (Figure 3). In the article, it was decided to investigate the causes of this corrosion and propose appropriate remedial measures.

RESULTS OF THE CALCULATIONS

The immediate cause of tank leakage is stress corrosion cracking, where the tank stresses are concentrated. Therefore it is necessary to establish its causes, i.e. loads causing these concentrations. The loads of the tank structure that act on it
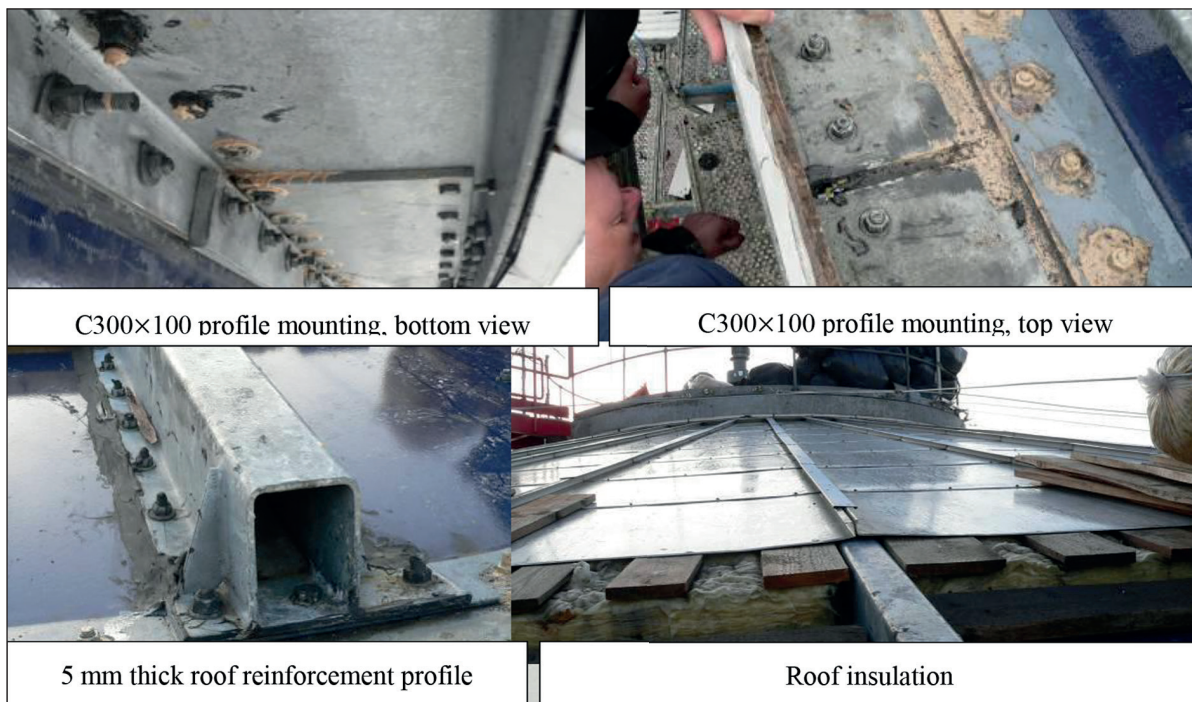

Figure 2. Connecting the cylindrical and conical parts reinforced with a C-profile 300,
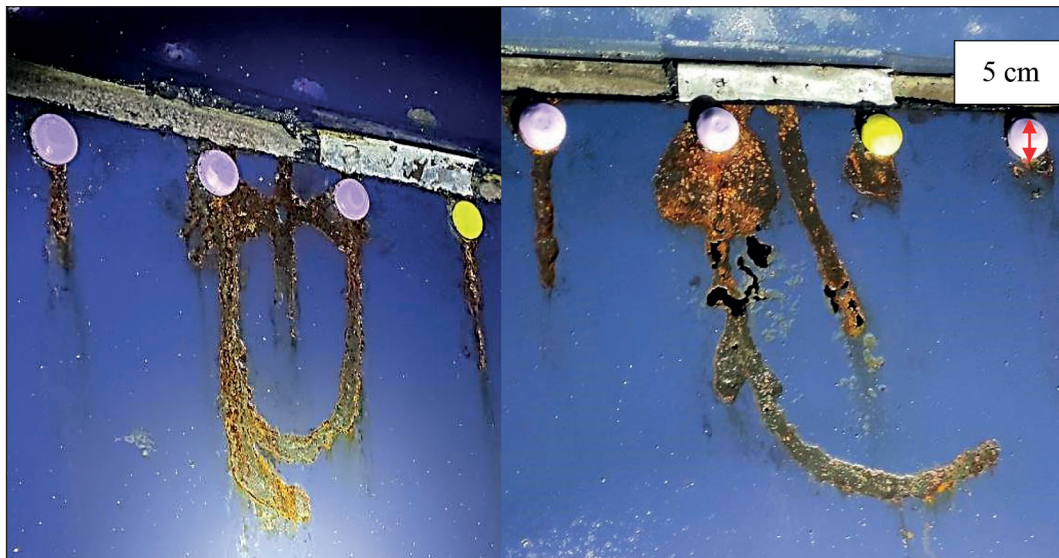reinforcement of the conical roof and thermal insulation with mineral wool

Figure 3. Electrochemical corrosion at the interface between the cylindrical part and the conical roof

constitute two groups. The first includes continuous static loads, which are sewage's weight and hydrostatic pressure. The second group consists of periodic loads of a variable nature, which are usually not considered at the design stage of a given technical object. They include:
- wind;
- the temperature difference in the elements of the tank structure;
- water hammer;
- other (soil settlement, shock loads).

To investigate the influence of individual loads on the stress state distributions in the tank structure, several numerical simulations were carried out using the FEM method for shell and solid models with different simplification levels. Depending on the model, 4 nodal shell or hexagonal solid elements were used. To find the cause of stress corrosion cracking, it was necessary to check which of the loads caused the stress concentration in the area of the channel section. For this reason, in the initial phase, the tank was tested as a whole, and in case of doubt, simulations were carried out on a more detailed model. About 15 variants of simulation were carried out until the most probable cause of corrosion was selected. In the article, it was decided to present only the most interesting cases. Since many of these variants had different mesh parameters and finite element types, finite element details were omitted. The following material data was adopted for the simulation and calculation of

stress distributions, strains and displacements in the fermentation tank:

Steel:
- Young's modulus $E = 2.1 \times 105$ MPa
- Poisson's ratio $n = 0.3$
- density $r = 7850$ kg/m3
- linear expansion $a = 2.1 \times 10{-}6$ K-1
- heat conductivity coefficient $l = 43$ W/(m×K)
- sewage density $rsew = 1000$ kg/m3
- air density $rair = 1.4$ kg/m3
- gravity $g = 9.81$ m/s2

Many simulations were carried out. However, due to their multiplicity, the article presents only selected results for the given loads, i.e.:
- simulation of hydrostatic load in sewage;
- simulation of constant overpressure gas load;
- simulation of the load on the hydrodynamic wind pressure;
- simulations for uncontrolled pressure build-up;
- simulation of the load resulting from the temperature difference.

The simulations of the hydrostatic load with sewage were made on the shell-solid model. The tank was loaded with the hydrostatic pressure of the sewage following the formula:

$$p = \rho_{sew} \cdot g \cdot z \qquad (1)$$

The HMH reduced stress values in such a loaded tank do not exceed 160 MPa and occur above the tank restraint. The maximum displacement at
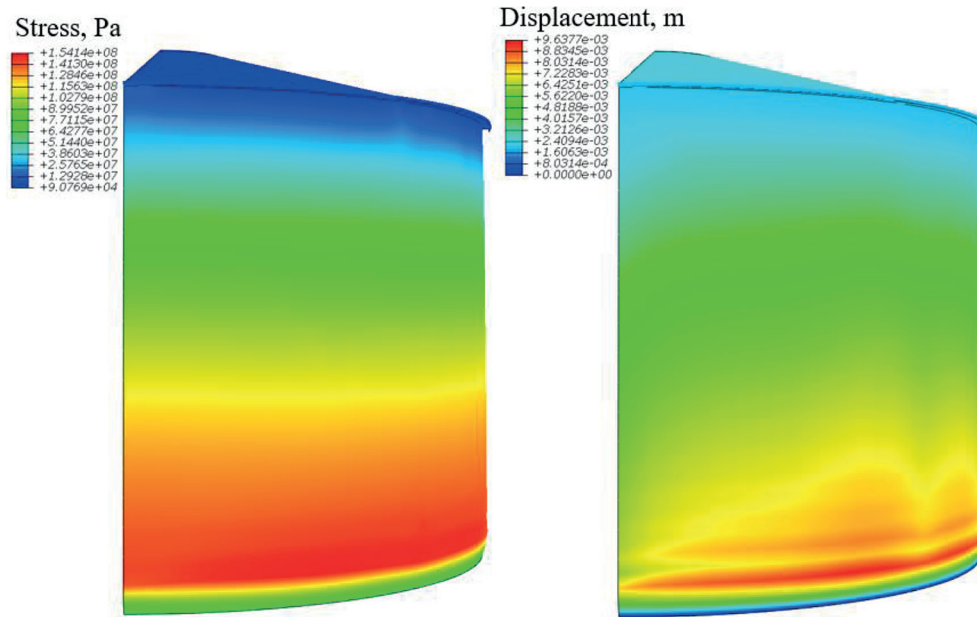
Figure 4. Distribution of reduced stresses according to the Huber-Mises hypothesis and displacement, hydrostatic pressure for rsew = 1000 kg/m3

this location is 9.6 mm (Figure 4). The stress distribution does not indicate where to connect to the roof, which makes it possible to rule out this as a cause of stress corrosion cracking.

The nominal working pressure of the tank is 3 kPa. Assuming a safety factor of 1.25, it was decided to load the tank with a pressure of 4 kPa. This imitates the situation during the leak test. The maximum value of the reduced stresses (HMH) is 20 MPa. The stress distribution does not indicate where to connect to the roof, which makes it possible to rule out this as a cause of stress corrosion cracking.

In another simulation, the tank was loaded with hydrodynamic air pressure during a hurricane that occurs on the Polish coast several times a year, assuming a wind speed of 120 km/h (33.3 m/s). Depending on humidity, atmospheric pressure and temperature, air density was adopted for extreme conditions. At pressure patm=100 kPa and temperature q = -25°C, it is approx r =1.4 kg/m3. The stagnation pressure for such assumptions is [13]:

$$p_{wind} = \frac{\rho_{air} \cdot v^2}{2} =$$
$$= \frac{1.4 \cdot (33.333)^2}{2} = 777.7 \, {}^N\!/_{m^2} \tag{2}$$

The value of this pressure is relatively small. Its direction was projected to the direction normal to the elements. In the wind-loaded tank, the stresses did not exceed 2 MPa. Their distribution also did not concentrate on the area of the roof sheathing, so it can't be assumed that this load caused corrosion stresses. The stress distribution does not indicate where to connect to the roof, which makes it possible to rule out this as a cause of stress corrosion cracking.

Calculations were also made, taking into account the uncontrolled increase in pressure, which is possible as a result of overfilling the tank or as a result of the failure of monitoring devices and the human factor. In the simulation, an increase in pressure of only 10 kPa was assumed, corresponding to 1 m of water column height. The obtained results (Figure 5) for this case indicate that the weakest design point of the tank is the area where a part of the cylindrical shell is connected to the conical roof. According to the simplified film theory of shells, the stress state in thin-walled shells is influenced by the radii of curvature [14]:

$$\frac{\sigma_1}{\rho_1} + \frac{\sigma_2}{\rho_2} = \frac{p}{g} \tag{3}$$

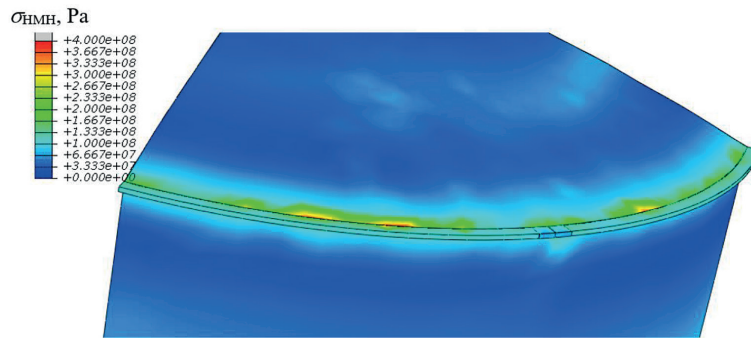for example, for a cylindrical vessel with a diameter D, thickness g, where the gas pressure is p,

Figure 5. Stress distribution sHMH caused by a pressure increase of 10 kPa. View from the outside

assuming that the axial and hoop stresses are different s1¹s2, the radii of curvature are:

$$\rho_1 = \frac{D}{2} \quad \rho_2 = \infty \qquad (4)$$

and the stress values are expressed by the formulas:

$$\sigma_1 = \frac{pD}{2g} \quad \sigma_2 = \frac{pD}{4g} \qquad (5)$$

According to this theory, for the construction of CFC's, the place of connection of a part of a cylindrical plating with a conical roof is a peculiarity, where the curvature radii change abruptly and are undefined, which results in stress concentration. In the above task, for the adopted calculation models, these stresses reach the value of 400 MPa, but in the actual tank, they may be lower.

In pressurized tanks, even with relatively low values, at the closure point of the cylindrical part of the so-called roof, sharp notches, i.e. abrupt changes in the radius of curvature, are avoided by using spherical and elliptical covers (Figure 6).

Figure 7 presents three exemplary simulations for similar steel tanks with a cylindrical structure, a diameter of 22 m, a height of 14 m, plating thickness of 10 mm, loaded from the inside with a pressure p = 10 kPa, closed with a conical, elliptical and spherical roof without joint reinforcement. This pressure in the cylindrical part, with a diameter of 22 m, causes stresses of 70 MPa. In the case of a tank closed with a spherical roof, the maximum Huber reduced stresses are just 10 MPa (Fig. 7c) and are located at the base of the tank. For a tank with an elliptical top, they are already 55 MPa (Fig. 7b) and occur in joining both parts, and for a conical roof in the same place, they reach the value of 433 MPa (Fig. 7a).

The influence of temperature change on the strength of the tanks was also considered.

During operation, mesophilic fermentation takes place inside the tank. Then the temperature inside ranges between 32–38°C [15]. On the other hand, in the area where the tank is located, frosts can reach -20°C, which causes even a 50-degree temperature difference. Thermal loads are caused by inadequate tank insulation, especially on the roof. There are many thermal bridges in the tank's geometrically "weak" elements, which causes the unfavourable distribution of thermal stresses. Apart from the C-profile, the outer surface of
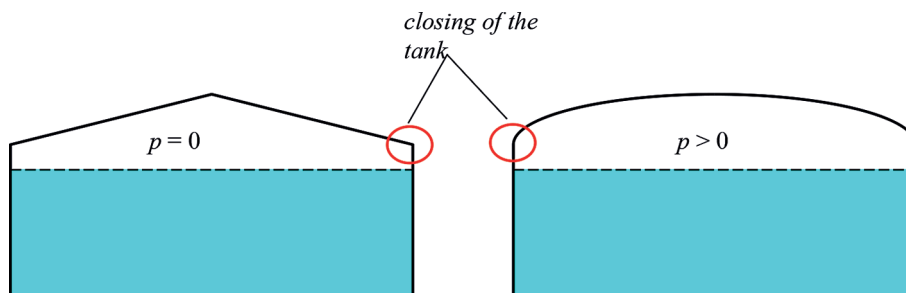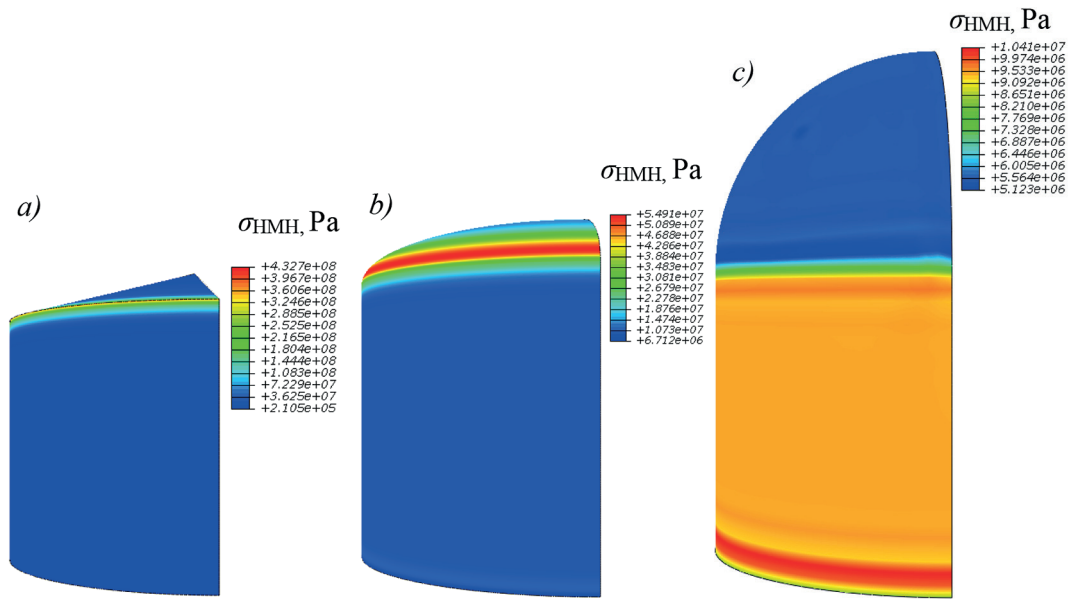

Figure 6. Closing of the tank

Figure 7. Influence of the shape of the cylindrical vessel closure on the distribution of reduced stresses

which is in contact with the surroundings, the place where temperature differences may cause cracks, is the roof, radially reinforced with steel profiles, 5 mm thick. The thermal insulation is arranged between the reinforcements, while the upper part of the profile has the ambient temperature, and in winter conditions, the roof sheathing will bend. The consequence of incorrect isolation is shown in Figure 8. It can be seen that the roof reinforcement is a thermal bridge between the tank interior and the environment. The differences can be seen more precisely compared to other roofs in the neighbourhood and on the top of the tanks excluded from the operation.

Due to the greater thickness of the roof and, in this case, maintaining the stiffness ratio in relation to the stiffening profiles, the values of thermal stresses amount to about 60 MPa, at a temperature difference of Dq = 30°C, and occur in the reinforcing profile, not in the roof sheathing.

At a temperature difference of Dq = 50°C, they increase to about 100 MPa in the reinforcement profiles, and in the plating, they reach values of the order of 20 MPa (Figure 9). These seemingly small values, due to the linear concentration, can cause corrosion and increase with the material loss. Moreover, in the places of joining the roof profile, additional local stress concentrations arise, which appear at the point of corrosion. The simulation results indicate that stresses up to 400 MPa may occur in the tested case.

Temperature changes have a significant impact on the stress state in the shell of the tank. The length of the ring made of channels is 69.7 m, so for Dq = 30°C, its shortening is 25 mm, for Dq = 40°C, its shortening is 33 mm, and for Dq = 50°C its shortening is 41 mm.

Numerical simulations have shown that the design of the CFC tanks is not very well suited to the conditions in which they operate. Large

Figure 8. View the working tank's roof after a snowfall and temperature –5°C
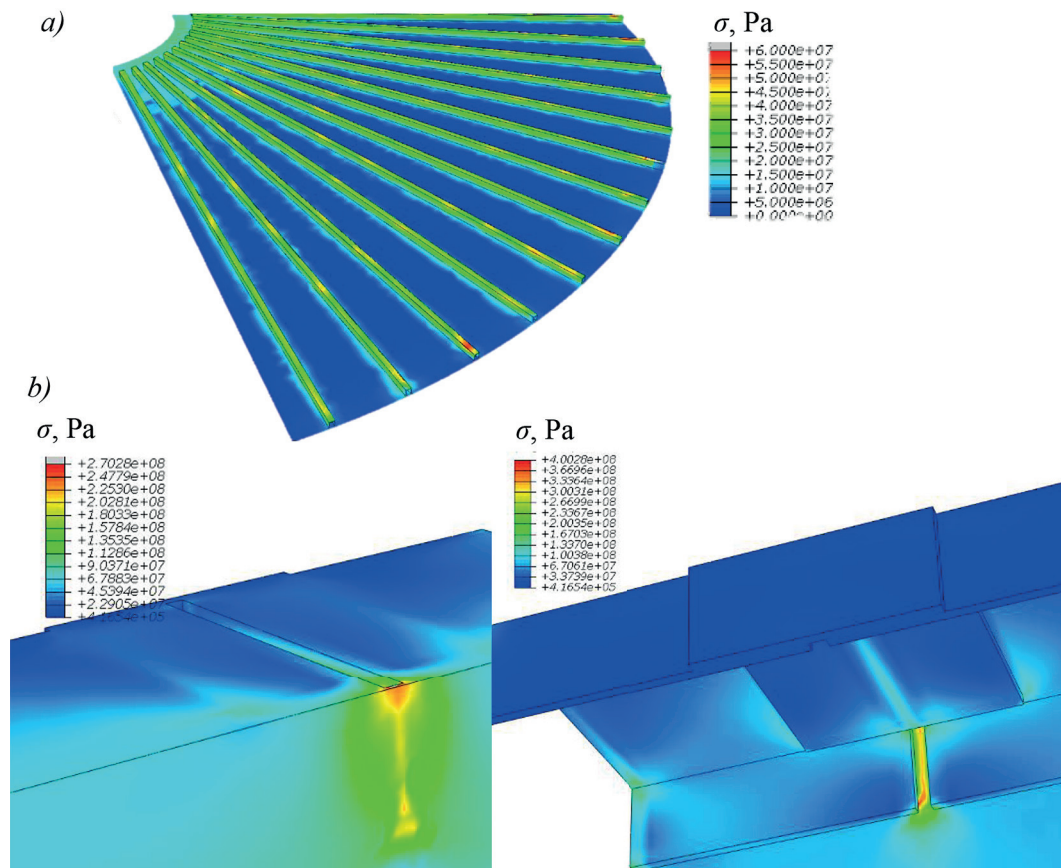
Figure 9. Stress distribution sHMH in the roof caused by the temperature difference Dq
= 30°C, a) view at roof reinforcement, b) view at channel profile mounting

temperature differences with existing thermal bridges cause significant stresses in the roof structure. This is due to the adaptation of the tank for other purposes to the fermentation tank. The connection of the cylindrical part with the conical roof is the place of stress concentration. Another problem is the inappropriate selection of the stiffness of the cooperating elements, i.e. connection of a rigid C-profile 300 with a thin sheet of 4 mm thickness. The most dangerous conditions for the tank are the thermal loads induced in the conical connection of the roof with the cylindrical part. Due to the tank's structure, it is unacceptable to load the internal part of the conical roof with pressures above 4 kPa. Such a situation may be caused by an increase in gas pressure above the liquid surface and (which is much more dangerous) an increase in the liquid level above the cylindrical part – overfilling the tank. As the nominal pressure in the tank is 3 kPa, an overfilling situation is rather rare. Hence, the most likely cause of tank failure is stress corrosion cracking due to temperature differential. The solution to the described problems may be the appropriate repair technology.

THE PROPOSED REPAIR TECHNOLOGY

When analyzing the causes of stress corrosion cracking, it was noticed that the roof joint should be strengthened and the transition between the roof and the tank walls softened. The repair contractor proposed a technology according to which it was necessary to remove the effects of corrosion, corrosion pits, supplement (fill) the corrosion cavities with composite materials, to strengthen the connection of the cylindrical part with the conical roof with Belzona composite materials [16], the purpose of which is to increase the strength of this joint, tightness and protection against electrochemical corrosion. The proposed repair technology will change the geometry of the connection of the cylindrical part with the conical roof. It seems reasonable to check how this change will affect the stress distribution in the tank structure. The geometric changes are presented in Figure 10.

The structure fragment repaired according to the proposed technology was subjected to numerical FEM simulation to determine the stress state. The simulation aims to compare the results
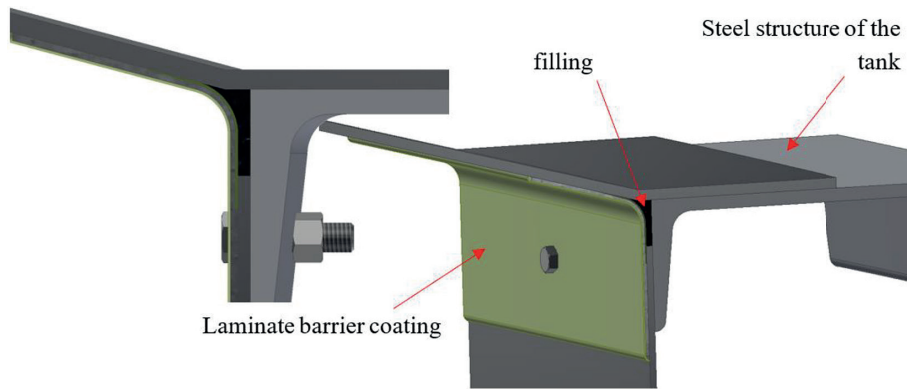
Figure 10. Visualization of tank repair

of the stress state after repair with the state of the structure before repair. Only a structure fragment, i.e. the connection of the cylindrical part with the conical roof, was analyzed. The object's symmetry was used, and the axisymmetric problem was solved (Figure 11). The cut-off of the analyzed fragment was completed with appropriate boundary conditions ensuring the continuity and symmetry of stresses.

All dimensions were adopted following the documentation of the tank. The appropriate material properties have been assigned to individual elements. The material constants for the filling are [17]:

- Young's modulus: 1200 MPa;
- Poisson's ratio 0.3.

For the barrier coating, the data for the laminate [14] was adopted and presented in Table 1.

The analyzed cross-section of the structure was discretized with flat, axisymmetric four-node elements and loaded from the inside with a
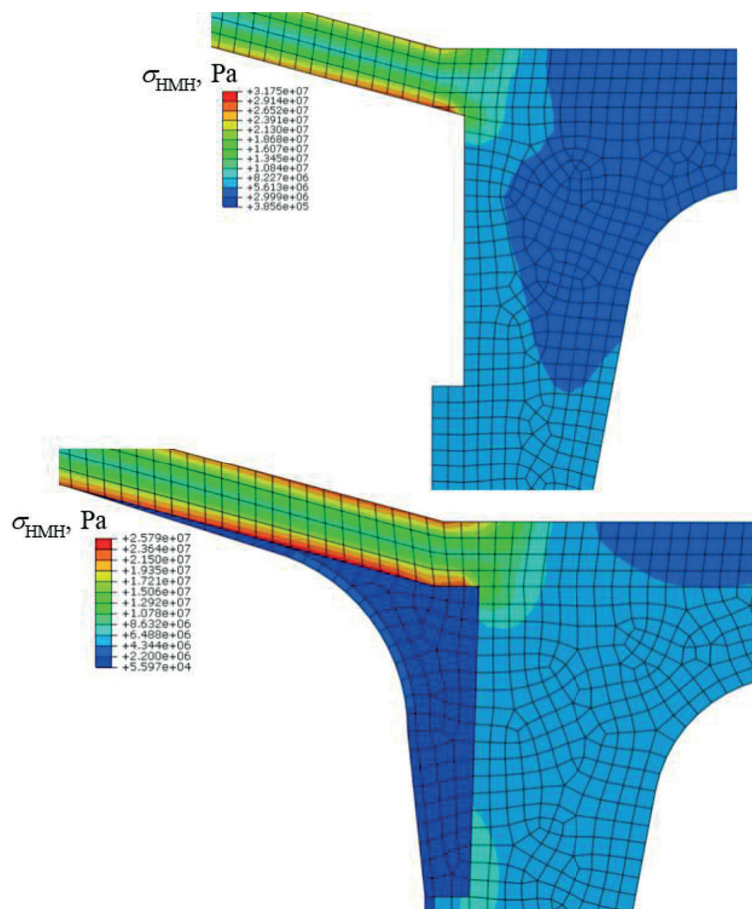

Figure 11. Reduced stresses HMH in the cross-section of the tank plating before and after repair

Table 1. Material constants for the laminate (E – Young's modulus, ν – Poisson's ratio, G – Kirchhoff modulus) [18]

E_x	E_y	E_z	v_{xy}	v_{yz}	v_{xz}	G_{xy}	G_{yz}	G_{xz}
Pa	Pa	Pa	-	-	-	Pa	Pa	Pa
$1.7989 \cdot 10^{10}$	$1.7989 \cdot 10^{10}$	$1.948 \cdot 10^{9}$	0.08	0.698	0.0756	$1.857 \cdot 10^{9}$	$2.235 \cdot 10^{8}$	$2.235 \cdot 10^{8}$

working gas pressure of 4 kPa. Figure 11 shows the reduced stresses of the HMH. In the structure before the repair, they reach the values of 31.8 MPa. In the structure after repair, they drop to 25.8 MPa, which is about a 19% decrease for the analyzed task. The stress value decreases the load on the channel section and, thus, the entire roof joint structure. The pressure distribution at the joint also changes, which avoids local stress concentration. Strengthening and rounding the interior allows for an increase in the inter-repair period but does not entirely solve the problem.

CONCLUSIONS

Biogas is an interesting alternative in the world of more expensive non-renewable energy sources. Its production, however, is costly and not consistently profitable. It also turns out that its collection can be troublesome under unfavourable conditions. Closed fermentation chambers are exposed to many loads. Factors such as wind, hydrostatic pressure and gas pressure are crucial for the durability of such chambers. Moreover, during biogas formation, significant temperature differences arise between the inside of the chamber and the atmosphere, leading to thermal stresses and stress corrosion cracking.

The conversion of a grain tank to a fermentation tank is economically viable. It seems, however, that the designers did not anticipate all the risks of such a modification. Grain products by themselves do not emit heat like the fermentation process. In addition, the chamber is located in a place of severe frost, which puts it under considerable stress due to the temperature difference. The internal shape of the tank is also essential. Sharp roof-wall connections can be destructive for pressure tanks, even with a slight overpressure (3 kPa).

The article assessed that temperature has the most significant influence on the formation of corrosion losses. However, it should be borne in mind that the synergy of all the described loads should be considered for the overall strength of the chambers. The proposed repair technology

allows for reducing stresses by about 19%. This reduction occurs due to the formation of an oval shape between the roof and the tank's walls. Due to the good adhesion to steel, the composites used ensure the tightness of the connection of the cylindrical part with the conical roof. It should be borne in mind that the tanks operate under load conditions close to the permissible loads. Therefore they should be protected against the possibility of exceeding these loads. It should consider changing the roof insulation, which will reduce the impact of thermal stresses in the winter.

REFERENCES

1. Balat M, Balat H. Biogas as a Renewable Energy Source–A Review. Energy Sources, Part A: Recovery, Utilization, and Environmental Effects 2009; 31: 1280–93. https://doi.org/10.1080/15567030802089565.

2. Biogas. Clarke Energy n.d. https://www.clarke-energy.com/applications/biogas/ (accessed October 9, 2022).

3. Jiang X, Sommer SG, Christensen KV. A review of the biogas industry in China. Energy Policy 2011; 39: 6073–81. https://doi.org/10.1016/j.enpol.2011.07.007.

4. Kougias PG, Angelidaki I. Biogas and its opportunities–A review. Front Environ Sci Eng 2018; 12: 14. https://doi.org/10.1007/s11783–018–1037–8.

5. Gdańska Infrastruktura Wodociągowo-Kanalizacyjna Sp. z o.o. Energia z zasobów odnawialnych, Materiał edukacyjny dla szkół ponadgimnazjalnych (Energy from renewable resources, Educational material for secondary schools – in Polish) 2013.

6. Gdańska Infrastruktura Wodociągowo-Kanalizacyjna Sp. z o.o. GIWK n.d. https://www.giwk.pl/infrastruktura/elementy-infrastruktury/elektrocieplownia-biogazowa/ (Accessed July 5, 2022).

7. Grzechowiak R, Bitner W. Obliczenia symulacyjne wybuchów w silosach zbożowych (Simulation calculations of explosions in grain silos – in Polish). Journal of Research and Applications in Agricultural Engineering 2011; 56: 58–63.

8. Hotała E. Historyczne konstrukcje stalowych zbiorników i silosów na Dolnym Śląsku (Histori-

cal structures of steel tanks and silos in Lower Silesia – in Polish). Builder 2020; 24; 4. https://doi.org/10.5604/01.3001.0013.8800.

9. Dylewski AT, Łogin W. Use of the finite element method to design the properties of shaped joints made of composite materials. Adv Sci Technol Res J 2018; 12: 59–64. https://doi.org/10.12913/22998624/86209.

10. Lonkwic P. Optimisation of the Lift Carrying Frame Construction by Using Finite Element Method. Adv Sci Technol Res J 2018; 12: 207–15. https://doi.org/10.12913/22998624/100499.

11. Szturomski Bogdan, Kiciński Radosław, Świątek Krzysztof, Jurczak Wojciech, Bohn Marek. Ekspertyza stanu konstrukcji zamkniętej komory fermentacyjnej ob. Nr 15.3 w oczyszczalni ścieków Gdańsk Wschód (Expertise of the construction condition of a closed fermentation chamber, object No. 15.3 in the Gdańsk East sewage treatment plant – in Polish). Gdynia: Akademia Marynarki Wojennej; 2013.

12. Szturomski Bogdan. Analiza wpływu geometrii elementów konstrukcyjnych i obciążeń eksploatacyjnych na stan wytężenia poszycia stalowego cienkościennego wielkogabarytowego zbiornika (Analysis of the impact of the geometry of structural elements and operational loads on the state of stress on the steel plating of a thin-walled large-size tank – in Polish). Zeszyty Naukowe Akademii Marynarki Wojennej 2011: 95–106.

13. Kiciński R, Jurczak W. Submarine Resistance Force Characteristics Determination after Modification of Depth Rudder System. Adv Sci Technol Res J 2021; 15: 1–9. https://doi.org/10.12913/22998624/125186.

14. Dyląg Z., Jakubowicz A., Orłoś Z. Wytrzymałość materiałów [Strength of materials – in Polish]. vol. 1 i 2. Warszawa: Wydawnictwo Naukowo Techniczne; 2007.

15. Fachagentur Nachwachsende Rohstoffe, Deutsches Biomasseforschungszentrum, Kuratorium für Technik und Bauwesen in der Landwirtschaft, Institut für Agrartechnologie und Biosystemtechnik, editors. Leitfaden Biogas: von der Gewinnung zur Nutzung. 7. Auflage. Rostock: Druckerei Weidner; 2016.

16. Konieczny J. Materiały konstrukcyjne okrętów (Ship Construction Materials). Kwartalnik Bellona n.d.

17. Belzona. Belzona 1111 (Super Metal). www.belzona.com n.d. https://www.belzona.com/en/products/1000/1111.aspx (accessed July 5, 2022).

18. Tham CY, Tan VBC, Lee HP. Ballistic impact of a KEVLAR® helmet: Experiment and simulations. International Journal of Impact Engineering 2008; 35: 304.